O.V. Yevdulov, D.V. Yevdulov

O.V. Yevdulov

Federal State Budgetary Educational Institution of Higher Professional Education "Dagestan State Technical University", 70, Imam Shamil avenue, Makhachkala, 367015, Russia

D.V. Yevdulov

THEORETICAL STUDIES OF A LAYER-STRUCTURED THERMOELECTRIC ELEMENT

This paper is concerned with a model of a layer-structured thermoelectric element and presents the results of its theoretical studies. The thermoelement model makes it possible to study the thermophysical and thermomechanical processes occurring in it on the basis of solving the unsteady-state equation of thermal conductivity, the equilibrium, the continuity and the Duhamel-Neumann equations for a multi-layered system by a numerical finite element method. The results are represented as two-dimensional and one-dimensional plots of temperature, thermomechanical stresses and deformations at different thermoelement points.

Key words: thermoelement, cooling plant, temperature field, thermomechanical stresses and deformations, model, numerical finite element method.

Introduction

A continuous and stable operation of a number of devices can be achieved only under the necessary temperature conditions created for them. As a rule, the temperature operating conditions of thermally loaded devices are assured by special cooling systems, cooling plants. The latter are rather versatile, complicated, can have considerable dimensions, mass and energy consumption. In many cases, mass, dimensions and reliability of thermal-control systems are not always comparable to the respective parameters of cooled objects, which is particularly relevant for microminiature devices with high specific thermal fluxes. In this case, the problem of temperature stabilization of such equipment can be solved by using thermoelectric devices as cooling plants, optimally matched with this equipment in the most important energy and weight-size parameters.

The basic element of any thermoelectric device is a semiconductor thermoelement the types of which are covered adequately in [1-3]. Among them one should mention thermocouple, anisotropic, eddy and short-circuited thermoelements, thermoelements working in a magnetic field and at high temperature gradients, as well as piezothermoelements. The most widespread is classical flat-topped embodiment of these elements, when electric current is supplied perpendicular to heat flux on their cold and hot junctions. However, in the design of relatively high-power small-size cooling plants (of more than 1 kW power) based on this type of thermoelement, it is relevant to assure their reliable operation during the entire cycle of cooled equipment operation.

Thus, the existing low-current thermopiles, when used in large quantities, offer insufficient reliability due to increasing number of thermoelements, and, accordingly, soldered connections, as well as low thermodynamic characteristics. Low-current flat-topped thermopiles in this respect are better, but due to the presence of large heat fluxes on the junctions they have low thermomechanical characteristics.

To improve them, copper connecting plates are most often used with lead damping pads [4] which owing to their elasticity relieve thermoelement legs from stresses, though the electrical and thermal contact resistance is simultaneously increased. With low temperature differences, split connecting plates are sometimes used [5], with their thin jumpers offering elasticity and a low electric resistance due to their small length. In a number of designs, application has been found by compensated connecting plates and plates with different length on the cold and hot thermoelement sides [4]. Both designs call for the presence of increased gaps between thermoelement legs, which increases the value of heat flux from the hot to cold junctions through isolation and decreases useful cooling capacity.

Under such conditions, it seems advisable to employ layer-structured thermopiles (Fig.1) wherein the direction of electric current along thermolement does not change, the design is not rigid, owing to which the emerging thermomechanical stresses can be eliminated or reduced considerably.

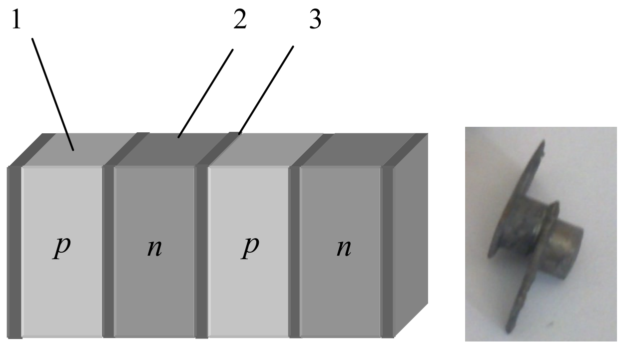

Fig.1. Design and external view of a layer-structured thermopile fragment.
1 and 2 – p- and n-type leg, 3 – connecting plates.

Dagestan Technical University has patented a number of solutions [6-14] implementing said concept that are different in the method of heat supply to and rejection from connecting elements, as well as in some other structural features.

The purpose of this paper is to develop a model and perform theoretical studies of a layer-structured thermoelement serving the basis for given technical solutions that will make it possible to optimize and determine the most advisable operating modes of the latter.

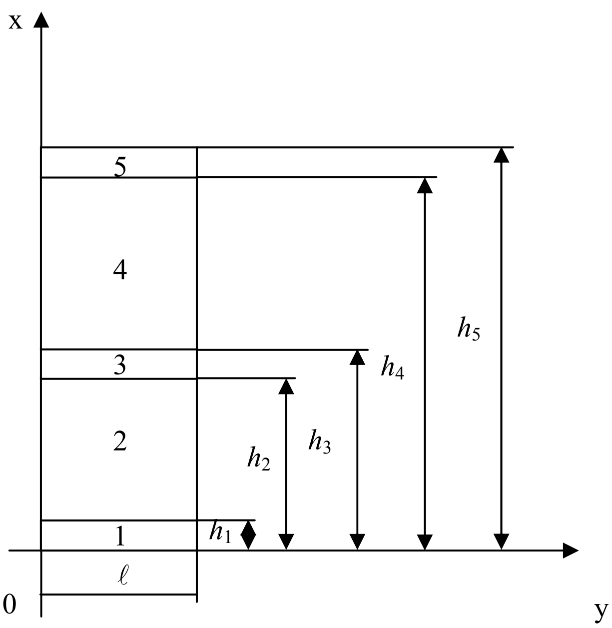

Fig.2. Calculation diagram of a layer-structured thermoelement.

Simulation of a layer-structured thermoelement includes calculation of its temperature field and thereupon determination of the respective thermomechanical characteristics.

Simulation of thermophysical processes and calculation of temperature field of a layer-structured thermoelement

In practice, in the majority of cases in operation of a thermopile, thermal isolation along its lateral surface is provided, except for contact surfaces with cooled object and heat rejection system. Therefore, with a sufficient degree of accuracy at simulation of a thermoelement one can consider a two-dimensional thermal conductivity problem. The calculation diagram for these conditions is shown in Fig. 2. The areas 1, 3 and 5 are connecting plates, 2 and 4 – thermoelectric material.

A system of differential heat transfer equations for this schematic is given by:

$$\lambda_1 \frac{\partial^2 T_1}{\partial x^2} + \lambda_1 \frac{\partial^2 T_1}{\partial y^2} + j^2\Omega_1 = C_1 \frac{\partial T_1}{\partial t},$$
$$\lambda_2 \frac{\partial^2 T_2}{\partial x^2} + \lambda_2 \frac{\partial^2 T_2}{\partial y^2} + j^2\Omega_2 = C_2 \frac{\partial T_2}{\partial t},$$
$$\lambda_3 \frac{\partial^2 T_3}{\partial x^2} + \lambda_3 \frac{\partial^2 T_3}{\partial y^2} + j^2\Omega_3 = C_3 \frac{\partial T_3}{\partial t}, \quad (1)$$
$$\lambda_4 \frac{\partial^2 T_4}{\partial x^2} + \lambda_4 \frac{\partial^2 T_4}{\partial y^2} + j^2\Omega_4 = C_4 \frac{\partial T_4}{\partial t},$$
$$\lambda_5 \frac{\partial^2 T_5}{\partial x^2} + \lambda_5 \frac{\partial^2 T_5}{\partial y^2} + j^2\Omega_5 = C_5 \frac{\partial T_5}{\partial t},$$

where λ_i is thermal conductivity coefficient, Ω_i is electric resistivity, j is electric current density, C_i is volumetric heat capacity, T_i is temperature, $i = 1,\dots, 5$, t is time.

The initial, boundary and matching conditions are as follows:

$$T_{1,2,3,4,5} = T_{amb} \text{ at } t = 0,$$
$$\lambda_1 \frac{\partial T_1}{\partial x} = \beta_{hr}\left(T_1 - T_{hr}\right) \text{ at } x = 0,\ 0 < y < \ell,$$
$$\lambda_1 \frac{\partial T_1}{\partial x} = \lambda_2 \frac{\partial T_2}{\partial x} + \alpha_{12} j T_2 \text{ at } x = h_1,\ 0 < y < \ell,$$
$$\lambda_2 \frac{\partial T_2}{\partial x} - \alpha_{23} j T_2 = \lambda_3 \frac{\partial T_3}{\partial x} \text{ at } x = h_2,\ 0 < y < \ell,$$
$$\lambda_3 \frac{\partial T_3}{\partial x} = \lambda_4 \frac{\partial T_4}{\partial x} - \alpha_{34} j T_4 \text{ at } x = h_3,\ 0 < y < \ell, \quad (2)$$
$$\lambda_4 \frac{\partial T_4}{\partial x} + \alpha_{45} j T_4 = \lambda_5 \frac{\partial T_5}{\partial x} \text{ at } x = h_4,\ 0 < y < \ell,$$
$$\lambda_5 \frac{\partial T_5}{\partial x} = \beta_{hr}\left(T_5 - T_{hr}\right) \text{ at } x = h_5,\ 0 < y < \ell,$$
$$\lambda_1 \frac{\partial T_1}{\partial y} = \beta\left(T_1 - T_{amb}\right) \text{ at } y = 0,\ \ell,\ 0 \le x \le h_1,$$
$$\lambda_2 \frac{\partial T_2}{\partial y} = \beta\left(T_2 - T_{amb}\right) \text{ at } y = 0,\ \ell,\ h_1 < x \le h_2,$$
$$\lambda_3 \frac{\partial T_3}{\partial y} = \beta\left(T_3 - T_{amb}\right) \text{ at } y = 0,\ \ell,\ h_2 < x \le h_3,$$
$$\lambda_4 \frac{\partial T_4}{\partial y} = \beta\left(T_4 - T_{amb}\right) \text{ at } y = 0,\ \ell,\ h_3 < x \le h_4,$$
$$\lambda_5 \frac{\partial T_5}{\partial y} = \beta\left(T_5 - T_{amb}\right) \text{ at } y = 0,\ \ell,\ h_4 < x \le h_5,$$

where T_{amb} is ambient temperature, α is the Seebeck coefficient, β is coefficient of heat exchange with the environment, β_{hr} is coefficient of heat exchange with heat rejection system, T_{hr} is temperature of heat rejection system.

The system of equations (1) with the respective initial and boundary conditions (2) was solved with the use of finite element method.

Figs. 3, 4 show, accordingly, a two-dimensional temperature field of a layer-structured thermoelement, as well as a distribution of heat flux density on reaching the steady-state mode. As the initial data there were used: $\lambda_1 = \lambda_3 = \lambda_5 = 395$ W/(m·K), $\lambda_2 = \lambda_4 = 1.5$ W/(m·K), $\rho_1 = \rho_3 = \rho_5 = 0.0172 \cdot 10^{-6}$ Ohm·m, $\rho_2 = \rho_4 = 10.65 \cdot 10^{-6}$ Ohm·m, $C_1 = C_3 = C_5 = 383$ J/(kg·K), $C_2 = C_4 = 123$ J/(kg·K), $T_{amb} = 293$ K, $T_0 = 291$ K, $\alpha = 0.2 \cdot 10^{-3}$ V/K, $\beta = 10$ W/(m^2·K), $T_{hr} = 291$ K, $\beta_{hr} = 70$ W/(m^2·K).

The value of heat flux was found from the ratio:

$$F_{xi} = \lambda_i \frac{\partial T_i}{\partial x}, \; F_{yi} = \lambda_i \frac{\partial T_i}{\partial y}, \text{ where } i = 1,\ldots,5.$$

Figs. 5-6 show, accordingly, the distribution of thermoelement temperature along its longitudinal axis at different supply current values, as well as a variation of temperature in time at different points of a layer-structured thermoelement.

As it follows from the resulting data, with the use of a layer-structured thermoelement one can obtain a considerable temperature difference between the cold and hot connecting plates with a large heat flux value. Thus, at temperature difference between connecting plates 47 K, heat flux on the cold junction of thermoelement, proportional to its cooling capacity, is of the order of 18000 W/m^2, which corresponds at given thermoelement geometry to supply current 140 A. With a decrease in supply electric current, the value of heat flux on the cold junction of thermoelement and temperature difference between its junctions are also reduced. In so doing, the reduction of thermoelement supply current from 140 A to 80 A reduces temperature difference between thermoelement junctions from 47 K to 31 K, consequently heat flux on the cold junction is reduced from 18000 W/m^2 to 12000 W/m^2.

Fig. 6 shows the variation of temperature of the cold and hot connecting plates, as well as different points of thermoelement leg in time at supply current 140 A. According to the represented data, the temperature at above points reaches the steady-state mode in about 900 sec. This fact is related to sufficiently large overall dimensions of thermoelement. With the thickness of connecting plates 2 mm and thermoelement legs height 4 mm, the cross-section area is $400 \cdot 10^{-6}$ m^2. In so doing, as it follows from the calculated data, it would be advisable to provide for heat rejection not only from the hot connecting plates, but also from the adjacent surface of thermoelement legs. In this design it is possible to propose additional heat rejection from about 1/3 of thermoelement lateral surface.

Simulation of thermomechanical processes in a layer-structured thermoelement

To estimate thermomechanical characteristics of a layer-structured thermoelement, calculation of mechanical stresses and deformations emerging in it due to thermal expansion of materials has been made.

The relations between mechanical stresses σ_x, σ_y, τ_{xy} and deformations ε_x and ε_y are given by the Duhamel-Neumann relations:

$$\varepsilon_x = \frac{1}{E}(\sigma_x - \nu\sigma_y) + \gamma T,$$

$$\varepsilon_y = \frac{1}{E}(\sigma_y - \nu\sigma_x) + \gamma T,$$

$$\gamma_{xy} = \frac{2(1+\nu)}{E}\tau_{xy},$$

where E is Young's modulus, ν is the Poisson coefficient, γ is linear expansion coefficient, indexes x, y, xy define the direction of values action, whereby index xy means the diagonal pattern of values action.

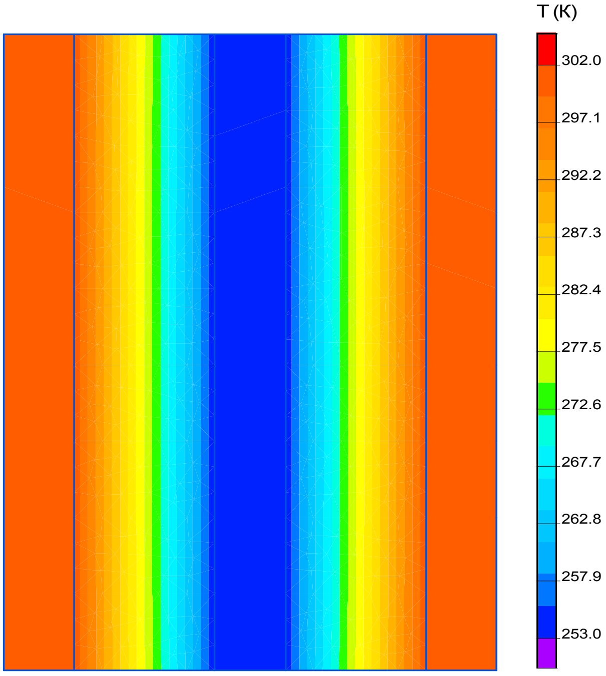

Fig.3. Temperature field of a layer-structured thermoelement.

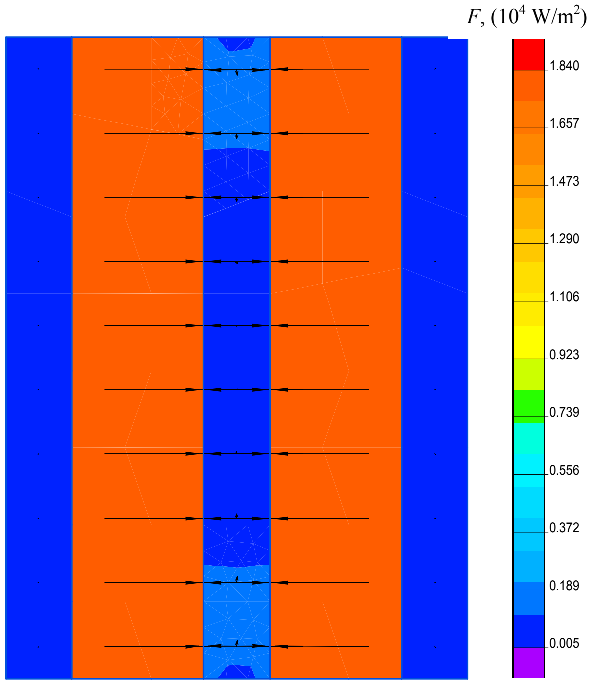

Fig.4. Thermal flow pattern in a layer-structured thermoelement.

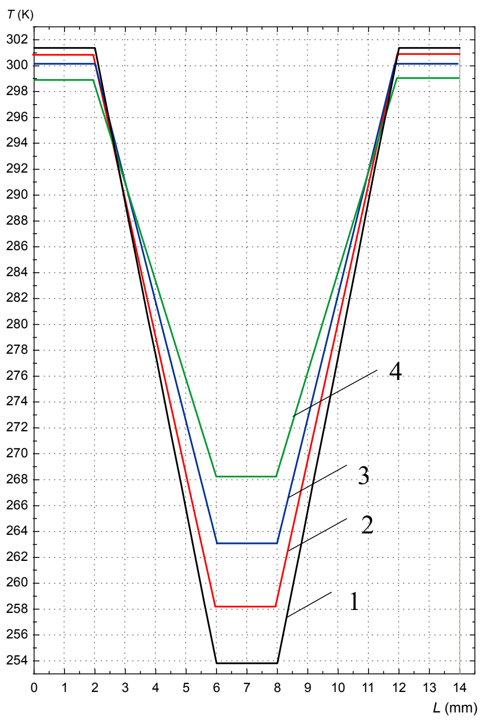

Fig. 5. Temperature distribution along the longitudinal axis of a layer-structured thermoelement at different supply current values: 1 – 140 A, 2 – 120 A, 3 – 100 A, 4 – 80 A.

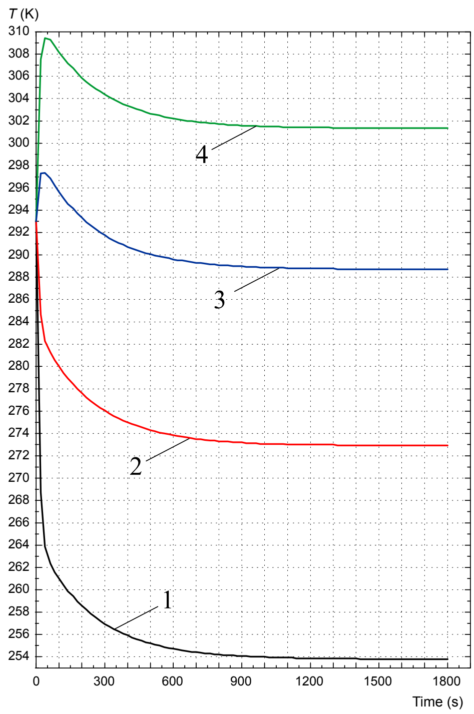

Fig. 6. Temperature variation at different points of a layer-structured thermoelement along the longitudinal axis in time: 1 – cold connecting plate, 2 – thermoelement leg at a distance of 1.5 mm from the cold connecting plate, 3 – thermoelement leg at a distance of 1.5 mm from the hot connecting plate, 4 – hot connecting plate.

Deformation ε_z is determined by means of ε_x and ε_y by the formula

$$\varepsilon_z = \frac{\nu}{\nu-1}(\varepsilon_y + \varepsilon_y) + \frac{1+\nu}{1-\nu}\gamma T .$$

When solving a plane thermoelasticity problem, the unknown stress values are assumed as σ_x, σ_y and τ_{xy}.

In the state of plane stress one can write

$$\nabla^2\left(\sigma_x + \sigma_y\right) + E\gamma\nabla^2 T = 0 .$$

Partial solution of thermoelasticity problem is given by:

$$\sigma_x^{(T)} = -2G\frac{\partial^2\Phi}{\partial y^2},\ \sigma_y^{(T)} = -2G\frac{\partial^2\Phi}{\partial x^2},\ \tau_{xy}^{(T)} = 2G\frac{\partial^2\Phi}{\partial x\partial y}, \tag{3}$$

$$G = \frac{E}{2(1+\nu)} .$$

For the state of plane stress we have

$$\nabla^2\Phi = \left(1+\nu\right)\alpha T , \tag{4}$$

where Φ is thermoelastic dislocation potential.

For the steady-state temperature fields:

$$\nabla^2 T = \frac{\partial^2 T}{\partial x^2} + \frac{\partial^2 T}{\partial y^2} = 0 ,$$

therefore, application of operator ∇^2 to Eq. (4) can yield

$$\nabla^2\nabla^2\Phi = \frac{\partial^4\Phi}{\partial \mathrm{x}^4} + 2\frac{\partial^4\Phi}{\partial \mathrm{x}^2\partial y^2} + \frac{\partial^4\Phi}{\partial y^4} = 0 . \tag{5}$$

Thus, if thermoelastic dislocation potential is found from Eq. (5), then stresses are found by simple differentiation in conformity with formula (3).

Due to the fact that elastic dislocation potential gives only partial solution, stresses (3) obtained with its help in the general case will not satisfy homogeneous boundary conditions.

Therefore, to free the boundary from the external effects, one must apply such a solution of elasticity theory equations which on the body surface will give stresses equal in value and opposite in sign to those that follow from Eq.(3).

Solution of this problem can be found through the Airy stress function by the formulae:

$$\sigma_x^{(P)} = \frac{\partial^2\varphi}{\partial y^2},\ \sigma_y^{(P)} = \frac{\partial^2\varphi}{\partial x^2},\ \tau_{xy}^{(P)} = -\frac{\partial^2\varphi}{\partial x\partial y}, \tag{6}$$

where φ is a biharmonic function.

The final solution of thermoelastic problem can be obtained by summation of Eqs. (3) and (6):

$$\sigma_x = \sigma_x^{(T)} + \sigma_x^{(P)} = \frac{\partial^2\left(\varphi - 2G\Phi\right)}{\partial y^2},$$

$$\sigma_y = \sigma_y^{(T)} + \sigma_y^{(P)} = \frac{\partial^2\left(\varphi - 2G\Phi\right)}{\partial x^2},$$

$$\tau_{xy} = \tau_{xy}^{(T)} + \tau_{xy}^{(P)} = \frac{\partial^2\left(2G\Phi - \varphi\right)}{\partial x\partial y}.$$

Introducing the Airy stress function related to stresses σ_x, σ_y, τ_{xy} by formulae similar to (6), and substituting them to (5) we obtain

$$\nabla^2\nabla^2\varphi + E\alpha\nabla^2 T = 0\,.$$

The general solution of this equation can be represented as

$$\varphi = \varphi^{(P)} + \varphi^{(T)}\,,$$

where $\varphi^{(P)}$ is a general solution of the biharmonic equation

$$\nabla^2\nabla^2\varphi^{(P)} = 0\,,$$

and $\varphi^{(T)}$ is a partial solution of equation

$$\nabla^2\varphi^{(T)} + E\alpha\nabla^2 T = 0\,.$$

Solution of thermal elasticity equations together with the boundary conditions defining the presence on all system faces of zero normal pressure, temperature distribution found when solving Eqs. (1)-(2), yields a two-dimensional pattern of mechanical stresses, deformations and dislocations.

The results of calculations are given in Figs. 7-8. The calculations were performed with the following initial data: $E = 1.2{\cdot}10^6$ N/m^2, $\nu = 0.3$ $\gamma = 22.2{\cdot}10^{-6}$ 1/K for thermoelectric material and $E = 1.2{\cdot}10^{11}$ N/m^2, $\nu = 0.34$ $\gamma = 16.8{\cdot}10^{-6}$ 1/K for copper connecting plates [15]. The ultimate strength of thermoelectric material is $1.0{\cdot}10^7$ N/m^2, of connecting plates – $3.2{\cdot}10^8$ N/m^2.

Fig. 7 shows a two-dimensional field of mechanical stresses for a layer-structured thermoelement with supply current 120 A, which corresponds to thermal flux value 16000 W/m^2.

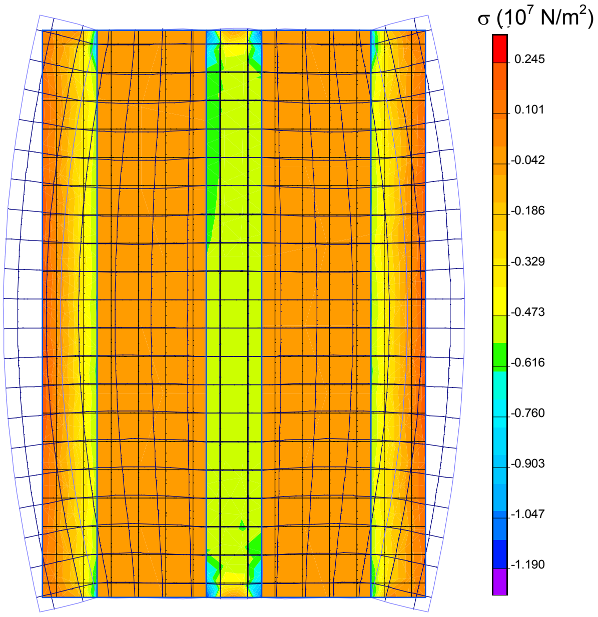

Fig. 7. Mechanical stress pattern in a layer-structured thermoelement.

From the foregoing data it follows that for the above thermoelement design the value of mechanical stresses does not go beyond the permissible values. Maximum load falls on points of contact between connecting plates and thermoelement legs. Here, mechanical load reaches the value of $0.9{\cdot}10^7$ N/m^2 for connecting plate. The greatest mechanical stresses in thermoelectric material do not exceed $0.2{\cdot}10^7$ N/m^2. Fig. 7 also depicts a deformed thermoelement boundary. As it appears from the figure, in the case of a layered thermoelement structure, the deformations are relatively small and are primarily due to elongation and extension of thermoelement on the sides, which is due to the absence of its rigid fixation along the edges. In so doing, maximum dislocation value according to calculated data does not exceed 0.18 mm.

For comparison, Fig. 8 shows a pattern of mechanical stresses under the same conditions for a classical flat-topped thermoelement. In this case deformations are rather large, and with a supply current of 120 A, without the use of special measures for reduction of thermomechanical loads, the mechanical loads exceed the respective ultimate strength of material.

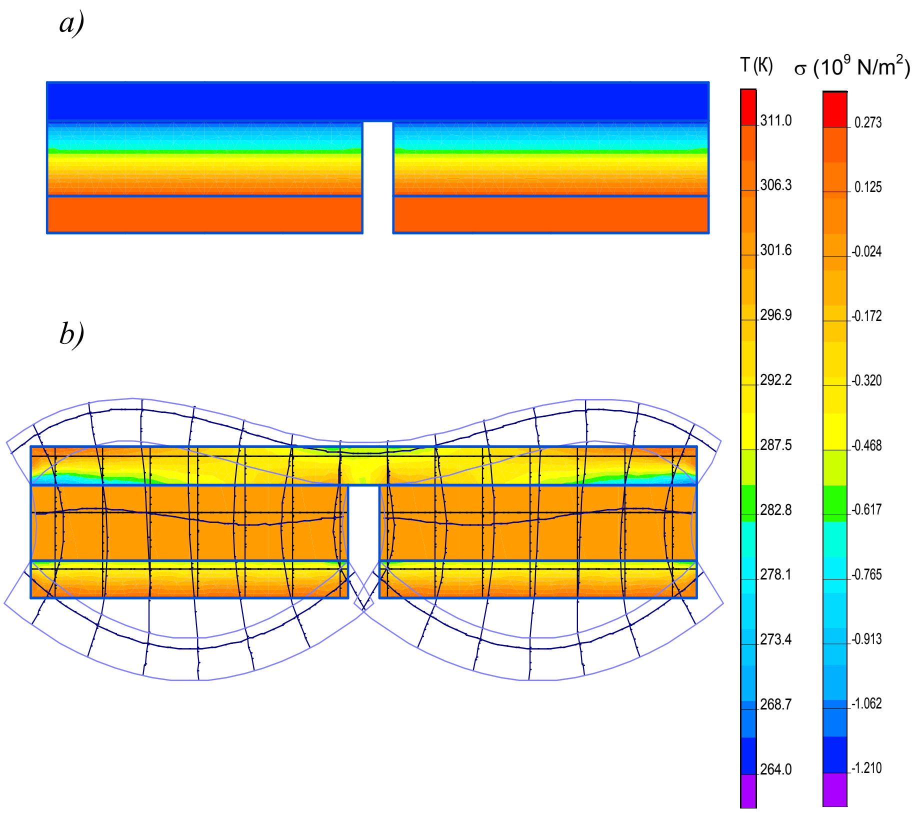

Fig. 8. Temperature field (a) and mechanical stress field (b) of a classical flat-topped thermoelement structure.

For instance, for connecting plates in conjunction with thermoelement leg the value of mechanical stress is above $7{\cdot}10^8$ N/m^2, which exceeds more than twice the ultimate strength of copper, for thermoelectric material the relation between mechanical loads and ultimate strength in this case is even higher. In so doing, in conformity with the calculations, it was established that for given thermoelement structure the largest supply current without excess of permissible value of mechanical loads in the system is electric current that does not exceed 82 A, i.e. almost a factor of 1.7 lower than in the case of using a layered thermoelement for which maximum supply current as per calculation is 140 A.

Conclusions

On the basis of investigations performed, the following conclusions can be made:

1. In the design of relatively high-power small-size cooling systems based on thermopiles, difficulties emerge in assuring their reliable operation. In this case, when low-current thermopiles are used, the reliability is affected by a large number of thermoelements, and in the case of high-current thermopiles – by the presence of essential thermomechanical stresses.

2. To reduce the value of thermomechanical stresses and deformations in high-current thermopiles, it is advisable to design them in the form of a layered structure where the directions of

electric current and thermal flow coincide.

3. Simulation of a layer-structured thermoelement includes its temperature field calculation and determination of corresponding thermomechanical characteristics. In so doing, temperature field calculation of a layer-structured thermoelement is done on the basis of solving the unsteady-state thermal conductivity equation for a multi-layered system, and determination of mechanical stresses and deformations is done, accordingly, when solving the equilibrium, continuity and Duhamel-Neumann equations by finite element numerical method.

4. The results of theoretical investigations of a layer-structured thermoelement have demonstrated its definite advantages over a classical flat-topped thermoelement as regards thermomechanical characteristics at high supply currents.

References

1. L.I. Anatychuk, *Thermoelectricity. Thermoelectric Power Converters* (Kyiv, Chernivtsi: Institute of Thermoelectricity, 2003).
2. L.I. Anatychuk, Basic Elements of Thermoelectricity, *Proc. of IX Interstate Workshop "Thermoelectrics and Their Applications"* (Saint-Petersburg, 2004).
3. L.I. Anatychuk, On the Physical Models of Thermoelements, *J.Thermoelectricity* **1**, (2003).
4. B.S. Pozdnyakov, E.A. Kokteylev, *Thermoelectric Power Engineering* (Moscow: Atomizdat, 1974).
5. B.E.-Sh. Malkovich, Thermoelectric Modules Based on Bismuth Telluride Alloys, *Proc. of XI Interstate Workshop "Thermoelectrics and Their Applications"* (Saint-Petersburg, 2008).
6. *Patent RF № 2280919*. Thermopile / T.A. Ismailov, M.G. Verdiev, O.V. Yevdulov, 2006.
7. *Patent RF* № 2280920. Thermopi le / T.A. Ismailov, M.G. Verdiev, O.V. Yevdulov, 2006.
8. *Patent RF* № 2280921. Thermopile / T.A. Ismailov, M.G. Verdiev, O.V. Yevdulov, 2006.
9. *Patent RF* № 2270495. Method for Support of Thermopile Operation / T.A. Ismailov, M.G. Verdiev, O.V. Yevdulov, 2006.
10. *Patent RF* №2335036. Thermopile / T.A. Ismailov, M.G. Verdiev, O.V. Yevdulov, D.V. Yevdulov, 2008.
11. *Patent RF* № 2357330. Thermopile / T.A. Ismailov, M.G. Verdiev, O.V. Yevdulov, 2009.
12. *Patent RF* № 2380787. Thermopile / T.A. Ismailov, O.V. Yevdulov, D.V. Yevdulov, 2010.
13. *Patent RF* № 2379790. Thermopile / T.A. Ismailov, O.V. Yevdulov, D.V. Yevdulov, 2010.
14. *Patent RF* № 2417484. Thermopile / T.A. Ismailov, O.V. Yevdulov, D.V. Yevdulov, 2011.
15. A.I.Voronin, A.S.Osilkov, and T.A. Gorbatovskaya, On the Issue of Mechanical Strength of Thermoelement Legs Based on Bi_2Te_3, *Proc. of XI Interstate Workshop "Thermoelectrics and Their Applications"* (Saint-Petersburg, 2008).

Submitted 14.04.2015